Effects of the neutron spin-orbit density on the nuclear charge density in relativistic models

Haruki Kurasawa
Department of Physics, Faculty of Science, Chiba University, Chiba 263-8522, Japan

Toshio Suzuki
Department of Applied Physics, Fukui University, Fukui 910-8507, Japan,
and RIKEN, 2-1 Hirosawa, Wako-shi, Saitama 351-0198, Japan
(Received 9 May 2000; published 29 September 2000)

The neutron spin-orbit density contributes to the nuclear charge density as a relativistic effect. The contribution is enhanced by the effective mass stemming from the Lorentz-scalar potential in relativistic models. This enhancement plays an important role to explain the difference between the cross sections of elastic electron scattering off ^{40}Ca and ^{48}Ca which is not reproduced in the present nonrelativistic models. The spin-orbit density will be examined in more detail in electron scattering off unstable nuclei which would be available in the future.

PACS number(s): 21.10.Ft, 21.30.Fe, 21.60.−n, 25.30.Bf

In recent years, it has been shown that many of the nuclear ground-state properties are well reproduced by the Hartree-Fock calculations using the Skyrme effective forces (SHF) [1] and by the relativistic mean-field calculations (RMF) [2]. For a long time, however, the problem remains that SHF and RMF cannot explain the difference between the cross sections for elastic electron scattering from ^{40}Ca and ^{48}Ca. Since they are described as closed-shell nuclei, it was expected that the difference could be easily understood by SHF and RMF, but the problem is not yet solved.

In 1972, Bertozzi *et al.* [3] took into account effects of the neutron spin-orbit charge density as a relativistic correction to SHF. The relativistic correction was derived by expanding the Pauli current of the free nucleon in terms of $1/M$, M being the mass of the free nucleon. They found that the relativistic correction was not negligible, but not enough to explain the difference between the two cross sections. In 1976 Miller [4] analyzed the same data using RMF, but again could not reproduce the experimental data. The Pauli current made rather worse the agreement between his results and experiment. Since then, there have been no efforts to solve this problem, as far as the authors know [5].

Recently, new parameter sets of the Skyrme forces and the relativistic models have been proposed for better description of the nuclear ground-state properties. The purpose of this paper is to show that RMF with the new parameter sets can reproduce well the experimental data, but SHF still fails to explain them. Our relativistic models discussed below are in principle the same as Miller's, but we will make clear the relationship between the relativistic and nonrelativistic models. In the relativistic models the effective mass coming from the Lorentz scalar potential yields an additional spin-orbit charge density as a relativistic correction. This correction improves the agreement between experimental data and RMF results. We will also show that those effective-mass effects will be able to be explored in more detail, if electron scattering from unstable nuclei would become available.

We calculate the cross section for elastic electron scattering using phase shift analyses [6]. For this purpose we have to obtain the nuclear charge density, which is given by

$$\rho_c(r)=\int \frac{d^3q}{(2\pi)^3}\exp(-i\mathbf{q}\cdot\mathbf{r})\langle 0|\hat{\rho}(\mathbf{q})|0\rangle, \tag{1}$$

where $\mathbf{q}$ denotes the momentum transfer from the electron to the nucleus. In the relativistic theory, the ground-state expectation value of the time component of the nuclear current is given by

$$\langle 0|\hat{\rho}(\mathbf{q})|0\rangle=\langle 0|\sum_k \exp(i\mathbf{q}\cdot\mathbf{r}_k) \times\left(F_{1k}(\mathbf{q}^2)+\frac{\mu_k}{2M}F_{2k}(\mathbf{q}^2)\mathbf{q}\cdot\boldsymbol{\gamma}_k\right)|0\rangle, \tag{2}$$

where $F_{1k}(\mathbf{q}^2)$ and $F_{2k}(\mathbf{q}^2)$ stand for the Dirac and Pauli form factors of the nucleon, respectively, and μ_k the anomalous magnetic moment. The above equation is rewritten by using the Sachs form factor, $G_E(\mathbf{q}^2)$, as

$$\begin{aligned}\langle 0|\hat{\rho}(\mathbf{q})|0\rangle&=\int d^3x\,\exp(i\mathbf{q}\cdot\mathbf{x}) \times\sum_\tau\,[G_{E\tau}(\mathbf{q}^2)\rho_\tau(x)+F_{2\tau}(\mathbf{q}^2)W_\tau(x)]\\ &=\int d^3x\,d^3y\,\exp[i\mathbf{q}\cdot(\mathbf{x}+\mathbf{y})] \times\sum_\tau\,[G_{E\tau}(y)\rho_\tau(x)+F_{2\tau}(y)W_\tau(x)],\end{aligned} \tag{3}$$

where the sum of τ is performed with respect to the proton and the neutron, $\tau=p,n$. The functions, $G_{E\tau}(y)$ and $F_{2\tau}(y)$, are obtained by the inverse Fourier transformation of the Sachs and Pauli form factors, respectively. The nucleon density $\rho_\tau(x)$ and the spin-orbit density $W_\tau(x)$ are given by

$$\rho_\tau(r)=\langle 0|\sum_k\,\delta(\mathbf{r}-\mathbf{r}_k)|0\rangle, \tag{4}$$

$$W_\tau(r)=\frac{\mu_\tau}{2M}\left(-\frac{1}{2M}\nabla^2\rho_\tau(r)+i\nabla\cdot\langle 0|\sum_k \delta(\mathbf{r}-\mathbf{r}_k)\boldsymbol{\gamma}_k|0\rangle\right), \tag{5}$$

where the sum over k is performed up to Z for $\tau=p$ and up to N for $\tau=n$. By inserting Eq. (3) into Eq. (1), the nuclear charge density is given by

$$\rho_c(r)=\sum_\tau [\rho_{c\tau}(r)+W_{c\tau}(r)], \tag{6}$$

where the nucleon charge density $\rho_{c\tau}(r)$ and the spin-orbit charge density $W_{c\tau}(r)$ are written as

$$\rho_{c\tau}(r)=\frac{1}{r}\int_0^\infty dx\, x\rho_\tau(x)[g_\tau(|r-x|)-g_\tau(r+x)], \tag{7}$$

$$W_{c\tau}(r)=\frac{1}{r}\int_0^\infty dx\, xW_\tau(x)[f_{2\tau}(|r-x|)-f_{2\tau}(r+x)] \tag{8}$$

with

$$g_\tau(x)=\frac{1}{2\pi}\int_{-\infty}^{\infty} dq\, e^{iqx}G_{E\tau}(\mathbf{q}^2),$$

$$f_{2\tau}(x)=\frac{1}{2\pi}\int_{-\infty}^{\infty} dq\, e^{iqx}F_{2\tau}(\mathbf{q}^2).$$

In RMF the single-particle wave function is written as

$$\psi_{\alpha m}=\begin{pmatrix} i\dfrac{G_\alpha(r)}{r}\mathcal{Y}_{ljm} \\ \dfrac{F_\alpha(r)}{r}\dfrac{\boldsymbol{\sigma}\cdot\mathbf{r}}{r}\mathcal{Y}_{ljm}\end{pmatrix}.$$

The large and small components in the present model satisfy the Dirac equation:

$$\frac{dG_\alpha}{dr}=-\frac{\kappa_\alpha}{r}G_\alpha+[\varepsilon_\alpha-U_\tau(r)+M^*(r)]F_\alpha,$$

$$\frac{dF_\alpha}{dr}=\frac{\kappa_\alpha}{r}F_\alpha-[\varepsilon_\alpha-U_\tau(r)-M^*(r)]G_\alpha, \tag{9}$$

where $\kappa_\alpha=(-1)^{j-l+1/2}(j+1/2)$ denotes the eigenvalue of $-(1+\boldsymbol{\sigma}\cdot\boldsymbol{l})$, and $M^*(r)$ the nucleon effective mass given by

$$M^*(r)=M-U_s(r).$$

The Lorentz scalar potential $U_s(r)$ is due to the σ meson, while the Lorentz vector potential $U_\tau(r)$ is due to the ω and ρ mesons and photons in the present model. Then the nucleon density in Eq. (4) is given by

$$\rho_\tau(r)=\sum_\alpha \frac{2j_\alpha+1}{4\pi r^2}(G_\alpha^2+F_\alpha^2). \tag{10}$$

On the other hand, the spin-orbit density $W_\tau(r)$ in Eq. (5) is described as

$$W_\tau(r)=\frac{\mu_\tau}{M}\sum_\alpha \frac{2j_\alpha+1}{4\pi r^2}\frac{d}{dr}\left(\frac{M-M^*(r)}{M}G_\alpha F_\alpha + \frac{\kappa_\alpha+1}{2Mr}G_\alpha^2-\frac{\kappa_\alpha-1}{2Mr}F_\alpha^2\right). \tag{11}$$

The relationship between the relativistic model and nonrelativistic models is very clear. In nonrelativistic models, usually the neutron charge and spin-orbit charge densities are neglected in estimating the electron scattering cross section. Bertozzi *et al.* [3] took into account the neutron charge density and a part of the spin-orbit charge density in the nonrelativistic framework. Their spin-orbit density is obtained from Eq. (11) by setting $M^*(r)=M$ and neglecting F_α^2 term,

$$W_\tau(r)\approx\frac{\mu_\tau}{2M^2r^2}\frac{d}{dr}r\sum_\alpha\frac{2j_\alpha+1}{4\pi r^2}(\kappa_\alpha+1)\,G_\alpha^2 \tag{12}$$

$$\approx-\frac{1}{r^2}\frac{d}{dr}r\left\langle 0\left|\frac{\mu_\tau}{2M^2}\sum_k \delta(\mathbf{r}-\mathbf{r}_k)\boldsymbol{\sigma}_k\cdot\boldsymbol{l}_k\right|0\right\rangle. \tag{13}$$

We will show that the spin-orbit density due to the effective mass in Eq. (11) is very important in the relativistic model for reproducing the experimental data.

The nucleon form factors used in the present calculations are the dipole type as in Ref. [3], but obtained using more recent experimental data for the neutron [7]. The Sachs form factor for the proton is given by

$$G_{Ep}=\frac{1}{(1+r_p^2\mathbf{q}^2/12)^2},\quad r_p=\langle r^2\rangle^{1/2}=0.81\ \text{fm},$$

while the one for the neutron is given by

$$G_{En}=\frac{1}{(1+r_+^2\mathbf{q}^2/12)^2}-\frac{1}{(1+r_-^2\mathbf{q}^2/12)^2},$$

$$r_\pm^2=(0.9)^2\mp 0.06\ \text{fm}^2.$$

The Pauli form factors for the proton and the neutron are

$$F_{2p}=\frac{G_{Ep}}{1+\mathbf{q}^2/4M^2},\quad F_{2n}=\frac{G_{Ep}-G_{En}/\mu_n}{1+\mathbf{q}^2/4M^2}.$$

The values of the anomalous magnetic moment are given by $\mu_p=1.793$ and $\mu_n=-1.913$.

Now, we calculate the differential cross sections $\sigma(\theta)$ for elastic electron scattering off ^{40}Ca and ^{48}Ca and compare their difference $D(\theta)$ given by

$$D(\theta)=\frac{\sigma_{40}(\theta)-\sigma_{48}(\theta)}{\sigma_{40}(\theta)+\sigma_{48}(\theta)}, \tag{14}$$

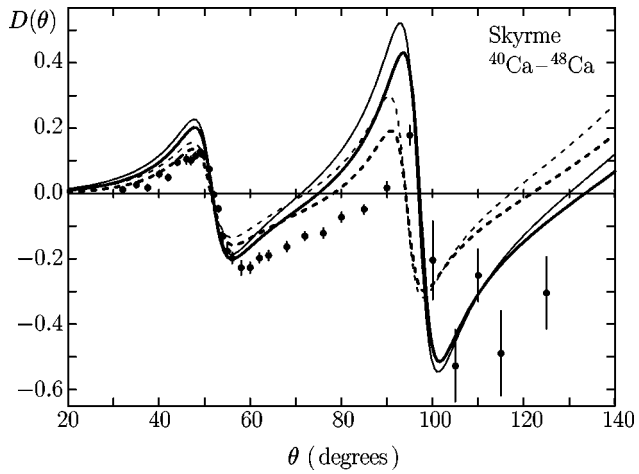

FIG. 1. The difference $D(\theta)$ for ^{40}Ca and ^{48}Ca given by Eq. (14) as a function of scattering angle θ for elastic electron scattering at 250 MeV. Numerical values are calculated by the nonrelativistic Hartree-Fock approximation with the Skyrme force I (solid curves) and SLy4 (dashed curves). The thin curves show the results with the only proton charge density, while the thick curves with the full charge density. Experimental data points are taken from Ref. [9].

with experiment. In Fig. 1 are shown the results of SHF. The solid and dashed curves show the results using the Skyrme force I [1] and SLy4 [8] without pairing correlations, respectively. The thin curves are obtained by taking into account the only proton charge density. When we include the neutron charge density and the proton and neutron spin-orbit charge density in Eq. (13), we obtain the thick curves. It is seen that the discrepancy between the theory and the experiment is reduced, in particular, at the electron scattering angle around $\theta=60°$ to 90°. This improvement is mainly due to the spin-orbit charge density from the neutrons in the $1f_{7/2}$ shell, but is not enough to explain the experimental data [9] in both Skyrme forces.

Figure 2 shows the results of RMF. The solid and dashed curves are calculated using the linear [10] and nonlinear

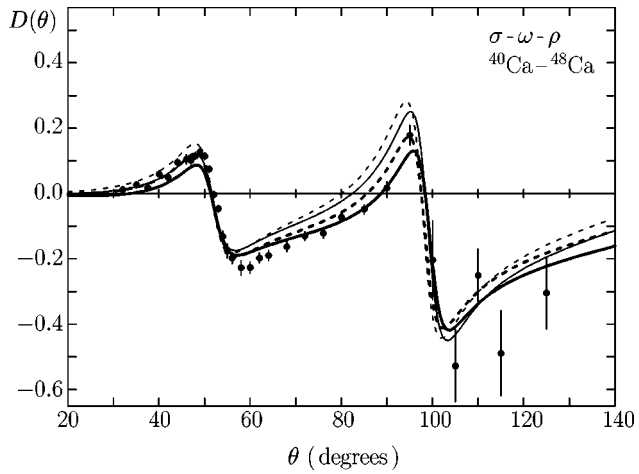

FIG. 2. Same as Fig. 1, for the numerical results of the relativistic models. The solid and dashed curves are calculated using the linear and nonlinear (NL-SH) σ-ω-ρ models, respectively.

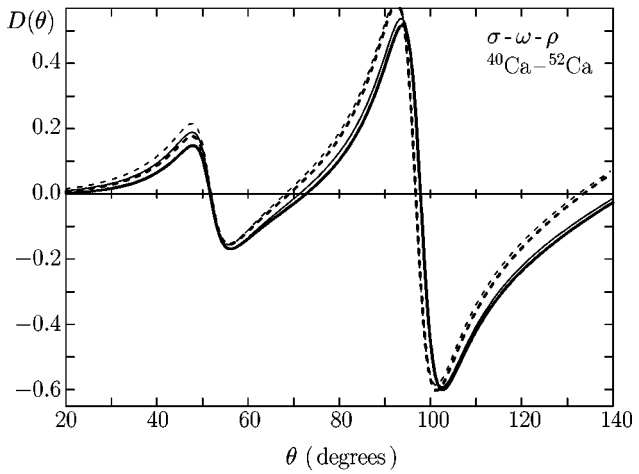

FIG. 3. Same as Fig. 2, for the difference as to ^{40}Ca and ^{52}Ca calculated by the relativistic models.

(NL-SH [11]) σ-ω-ρ models, respectively. The thin curves are obtained by taking into account the only proton charge density, while thick curves by the full density, Eq. (6). It is seen that in the relativistic models, the proton charge density itself is fairly improved, compared with the one in the nonrelativistic models. Moreover, the experimental data are almost reproduced by taking into account the neutron spin-orbit charge density enhanced by the effective mass. We note that in the linear σ-ω-ρ model, the spin-orbit density worsens a little the agreement with experiment in the range of $\theta=30°-50°$, but not in the nonlinear model. Detailed analysis of these two models is required in order to improve the agreement between theory and experiment.

We note that both in nonrelativistic and relativistic models, the center-of-mass correction to the cross section is negligible in Ca isotopes [12].

As seen in Eq. (11), the effects of the spin-orbit charge density appear, when the sub-shell is occupied by the neutrons. In closed shell nuclei, the effects disappear. Moreover, if protons also occupy the subshell as in ^{208}Pb, the proton and neutron spin-orbit densities almost cancel each other as in nonrelativistic model [3], since the anomalous magnetic moment of the proton has the opposite sign to that of the neutron. Another interesting result of the spin-orbit density is found in neutron rich nuclei. In Fig. 3 are shown the results with respect to ^{40}Ca and ^{52}Ca in the same designation as in Fig. 2. We see that effects from the spin-orbit charge density of the $1f_{7/2}$ neutrons are almost canceled by those from the $2p_{3/2}$ neutrons. Similar results are obtained in Zr isotopes [12]. The effect of the neutron spin-orbit charge density is enhanced in the cross section of ^{90}Zr, compared with the one of ^{80}Zr, but disappears in ^{96}Zr. It is interesting to observe experimentally these predictions of the relativistic model in electron scattering off unstable nuclei which is planned in RIKEN [13].

In conclusion, the effective mass due to the Lorentz scalar potential, which is a necessary ingredient of the relativistic models, enhances the neutron spin-orbit charge density in a peculiar way. The relativistic mean-field models with the enhanced density well explain the difference between the cross

sections of elastic electron scattering off ^{40}Ca and ^{48}Ca, which seems not to be reproduced in the present Skyrme Hartree-Fock calculations. Electron scattering off unstable nuclei is desirable in order to explore in more detail the spin-orbit density. More detailed discussions on the results of nonrelativistic and relativistic models will be published elsewhere [12].

The authors would like to thank Dr. T. Suda for useful discussions.

[1] D. Vautherin and D. M. Brink, Phys. Rev. C **5**, 626 (1972).
[2] B. D. Serot and J. D. Walecka, Adv. Nucl. Phys. **16**, 1 (1986).
[3] W. Bertozzi, J. Friar, J. Heisenberg, and J. W. Negele, Phys. Lett. **41B**, 408 (1972).
[4] L. D. Miller, Phys. Rev. C **14**, 706 (1976).
[5] C. J. Batty, E. Friedman, H. J. Gils, and H. Rebel, Adv. Nucl. Phys. **19**, 1 (1989); H. Feshbach, *Theoretical Nuclear Physics: Nuclear Reactions* (Wiley, New York, 1992), Chap. IX.
[6] D. R. Yennie, D. G. Ravenhall, and R. N. Wilson, Phys. Rev. **95**, 500 (1954).
[7] T. Eden *et al.*, Phys. Rev. C **50**, 1749 (1994); M. Meyerhoff *et al.*, Phys. Lett. B **327**, 201 (1994); S. Platchkov *et al.*, Nucl. Phys. **A510**, 740 (1990).
[8] E. Chabanat, P. Bonche, P. Haensel, J. Meyer, and R. Schaeffer, Nucl. Phys. **A635**, 231 (1998).
[9] R. F. Frosch *et al.*, Phys. Rev. **174**, 1380 (1968).
[10] C. J. Horowitz and B. D. Serot, Nucl. Phys. **A368**, 503 (1981).
[11] M. M. Sharma, M. A. Nagarajan, and P. Ring, Phys. Lett. B **312**, 377 (1993).
[12] H. Kurasawa, H. Madokoro, and T. Suzuki (unpublished).
[13] T. Suda (private communication).